PAPER

CrossMark
click for updates

Mechanical spectroscopy of retina explants at the protein level employing nanostructured scaffolds†

S. Mayazur Rahman,[abc] Andreas Reichenbach,[b] Mareike Zink‡*[a] and Stefan G. Mayr‡*[cd]

Development of neuronal tissue, such as folding of the brain, and formation of the fovea centralis in the human retina are intimately connected with the mechanical properties of the underlying cells and the extracellular matrix. In particular for neuronal tissue as complex as the vertebrate retina, mechanical properties are still a matter of debate due to their relation to numerous diseases as well as surgery, where the tension of the retina can result in tissue detachment during cutting. However, measuring the elasticity of adult retina wholemounts is difficult and until now only the mechanical properties at the surface have been characterized with micrometer resolution. Many processes, however, such as pathological changes prone to cause tissue rupture and detachment, respectively, are reflected in variations of retina elasticity at smaller length scales at the protein level. In the present work we demonstrate that freely oscillating cantilevers composed of nanostructured TiO_2 scaffolds can be employed to study the frequency-dependent mechanical response of adult mammalian retina explants at the nanoscale. Constituting highly versatile scaffolds with strong tissue attachment for long-term organotypic culture atop, these scaffolds perform damped vibrations as fingerprints of the mechanical tissue properties that are derived using finite element calculations. Since the tissue adheres to the nanostructures *via* constitutive proteins on the photoreceptor side of the retina, the latter are stretched and compressed during vibration of the underlying scaffold. Probing mechanical response of individual proteins within the tissue, the proposed mechanical spectroscopy approach opens the way for studying tissue mechanics, diseases and the effect of drugs at the protein level.

1. Introduction

Almost 60 years ago Heilbrunn stated: "In any attempt to interpret the machinery of a living cell, it is essential to know something about the mechanical properties of the protoplasm in the cell that is being investigated".[1] Since then the focus on the molecular structure and signaling mechanisms has explained many aspects of the cell function and pathology, but the mechanical properties of tissues and cells which play an

important role in embryologic development and diseases such as cancer[2] remain largely undefined.

As for mechanical properties, biological tissues and cells are viscoelastic systems that respond to external mechanical stimuli as a function of time scale and reveal characteristics ranging from purely elastic to fluid behavior.[3–7] Moreover, cells and tissues exhibit a rich dynamic behavior.[7,8] Hence, the stiffness of entire tissue and the elasticity of single cells determine if and how cells can migrate within the body,[9,10] *e.g.* during wound healing. Considering wounds affecting nerves and the central nervous system of the spinal cord, cells such as glial cells and fibroblasts often cause scar tissue which can cause permanent paraplegia because the injured nerve loses regenerability.[11] On the other hand the development of the nervous system is a complex dynamical process in which mechanical forces direct the growth and motion of neurons and the development of neurites which become axons and dendrites. In later stages tension of axons occurs which contributes to the development of neuronal networks and folding of the brain cortex.[5,12]

Another type of complex neuronal tissue is the vertebrate retina which is constantly exposed to several different types of mechanical stresses. For example, negative pressure is pulling

[a] *Soft Matter Physics Division, Institute for Experimental Physics 1, University of Leipzig, Linnéstr. 5, 04103 Leipzig, Germany. E-mail: zink@physik.uni-leipzig.de*
[b] *Paul Flechsig Institute for Brain Research, University of Leipzig, Liebigstr. 19, 04103 Leipzig, Germany*
[c] *Leibniz Institute for Surface Modification (IOM), Permoser Str. 15, 04318 Leipzig, Germany. E-mail: smayr@uni-leipzig,de*
[d] *Division of Surface Physics, Department of Physics and Earth Sciences, University of Leipzig, Leipzig, Germany*
† Electronic supplementary information (ESI) available. See DOI: 10.1039/c6sm00293e
‡ Contributed equally.

on the outer retinal surface due to constant pumps of fluid by the retinal epithelium from the subretinal space to the choroid.[13,14] Even the highly viscous vitreous body which is attached to the retina and lens assigns continuous shear forces at the retinal surface during every movement of the eye.[15] Thus, the mechanical properties of the adult mammalian retina play a crucial role in many pathological events such as retinoschisis[14] where the retina swells, and Müller cells are overstretched, become mechanically instable and rupture. Moreover, retinal detachment and/or macular hole formation may result from age-related events such as vitreous shrinkage and vitreous liquefaction.[15] Recently Mac Donald *et al.* showed that not only the entire retina but also Müller glial cells are under tension *in vivo* which can be considered as springs holding the retina together.[16]

When heading for characterization of cell and tissue mechanics it should be kept in mind that the underlying scaffold or substrate material often influences cellular behavior even though cell–substrate interactions take place on the nanometer length scale, *viz.* much smaller than the cells themselves. *In vitro* observations showed that neurons can sense nanometer cues which can also stimulate their behavior on unphysiological stiff substrates such as gold.[17] However, neuronal growth and development are highly influenced by the stiffness of the surrounding matter as well.[18]

Numerous studies on tissue mechanics, including the retina, employ scanning force microscopy (SFM) in which a tip or a bead with a diameter of a few micrometers is pressed into the tissue, while the resulting force is determined.[15] Even on smaller length scales, SFM has also been employed to assess many important biomechanical features of single biological polymers.[19–22] However, a combination of both the investigation of tissue mechanics with a statistically significant quantitative analysis technique of proteins on the nanometer length scale at the tissue-substrate interface is an almost impossible challenge with these techniques.

To address the mechanical properties of adult retina explants in terms of the frequency dependent elastic properties at the molecular length scale, we present a twofold study. First we show how fully elastic TiO_2 nanostructured templates are employed as tissue scaffolds for mechanical spectroscopy of retina explants. By measuring the intrinsic vibration modes of the scaffolds with the retina on top in a home-built setup, the interaction of the tissue in contact with TiO_2 nanotopography is directly reflected in a change of vibration behavior. Second, we employ our assay to study the mechanical properties of the adult mammalian retina at the tissue–scaffold interface at molecular scales. In fact, the strong adhesion of the tissue to the scaffold surface results from the attachment of biomolecules, *viz.* proteins and polymers on the photoreceptor side of the retina, which are exposed to mechanical load/unload cycles in the course of scaffold vibrations. The acting intramolecular forces quantify the elastic properties of the retina at the tissue–scaffold interface at the nanometer length scale which are directly measured *in situ*.

Since our novel biotechnological approach can be employed for many different types of tissues, the investigation of tissue mechanics on sub-cellular and even smaller length scales offers new possibilities to study the effect of drugs, or structural variations

during pathological changes. Here especially the photoreceptor side of the retina, which is the focus of our study, is of great importance, as the interphotoreceptor (IPR) matrix – connecting the outer photoreceptor segments with the retinal pigment epithelium – is often involved in retinal detachment and loss of vision.[23–25] The underlying pathological changes of the IPR matrix occur at the molecular level, *i.e.*, in the chondroitin sulfate proteoglycan core proteins which are responsible for retinal adhesion.

2. Experimental

2.1. Nanostructured scaffold fabrication

Nanostructured scaffolds are stable, but elastic and flexible materials comprising parallel aligned nanometer-size tubes of TiO_2 which were synthesized by electrochemical anodization using a titanium-foil (Ti) as an anode and a platinum-mesh as a cathode according to Fischer and Mayr.[26] Ti foil (99.6+% purity, Advent Ltd) of 100 μm thickness was cut according to the desired sample size and cleaned by sonicating in isopropanol and deionized water for 10 minutes successively. Prior to anodization, the electrolytes were prepared under the hood with ventilation by using ethylene glycol (Merck KGaA), 0.3 wt% ammonium fluoride (Merck, EMSURE-ACS) and 2% distilled water. The Ti sheet was attached to an alligator clip opposite the platinum mesh (Advent Research Material LTD: 99.9%, 52 mesh per inch; 25×25) and placed inside a beaker with the electrolyte solution inside. The distance between the titanium plate and the platinum mesh was adjusted to 4–5 cm. The anodization process was run under 50 V for 60 minutes at room temperature. Subsequently, the sample was taken out of the electrolyte and cleaned with ethylene glycol (EG). In a next step, EG was removed from the sample by gentle stream of nitrogen and then baked in an oven at 40–43 °C overnight. The resulting TiO_2 scaffold was removed from the oven the next day and cleaned by sonicating in deionized water for 10–15 minutes. After drying in a nitrogen stream, the scaffold was characterized by using a field emission scanning electron microscope (FESEM; Zeiss Ultra 55).

The TiO_2 scaffolds display a self-assembled, free standing pore structure with a diameter of around 70 nm and a wall thickness of about 6 nm confirmed by electron microscopy. The tubes have an average length of 5.9 μm and are formed on top and bottom sides of an 88.2 μm thick titanium sheet. The entire scaffolds had a width of 5 mm and various lengths ranging from 18.4–25.4 mm with an additional 5 mm length for clamping the reed into a holder.

2.2. Preparation of retinal specimens and culture on TiO_2 scaffolds

Adult guinea pig retina wholemounts were employed for tissue culture and investigation of mechanical properties. Adult guinea pigs were handled in accordance with the European Council Directive 86/609/EEC and German guidelines for welfare of experimental animals (Tierschutzgesetz). Experiments were approved by the local authorities (Landesdirektion Sachsen, permit numbers T18/12A and T09/13).

Isolation of the retina was performed in a sterile room committed to primary culture experiments. Cleaning of the

eye was done in a Petri dish containing phosphate buffer saline (PBS) under a dissecting microscope to get rid of hair and the connective tissue remnants attached on the surface. Equatorial sectioning of an eyeball was started from about 2 mm behind the cornea by using scalpel, eye scissors and forceps. After removal of the lens, the retina remained attached to the vitreous. Therefore, the whole retina together with the vitreous body was placed as a sandwich between a previously prepared folded filter paper. After 30–40 seconds the filter paper was removed from the specimen to achieve a wholemount of fresh retina devoid of vitreous.

For mechanical spectroscopy adult guinea pig retina explants were punched with a circular blade of 3.74 mm diameter and placed on top of the TiO_2 scaffold with the photoreceptor side down. As we have shown previously, TiO_2 nanotube scaffolds are ideal substrates for long-term culture of adult retina tissue.[27] Here a Petri dish was filled with the tissue culture medium (Ames medium, A1420, Sigma-Aldrich, Germany) with 10% horse serum (H 1270, Sigma-Aldrich, Germany) and 0.1% gentamicin (1357, Sigma-Aldrich, Germany) up to a level that it came into contact with the scaffold but did not cover the retina. Since the scaffolds are super-hydrophilic, culture medium automatically spreads and covers the entire surface with the tissue on top of the scaffolds. Fresh medium flows from the reservoir in the Petri dish to the top for ideal nutrient supply without perfusion systems (Fig. 1) (for more details see the study of Dallacasagrande et al.[27]). The whole setup was then incubated overnight at 37 °C and 5% CO_2.

2.3. Mechanical spectroscopy

Mechanical spectroscopy is an analysis technique to characterize the frequency-dependent mechanical properties of a material. Here a vibrating reed setup was designed (Fig. 2), in which a solid rectangular TiO_2 nanostructured scaffold acts as a vibrating reed onto which the retina explant is placed to study its mechanical response during vibration.
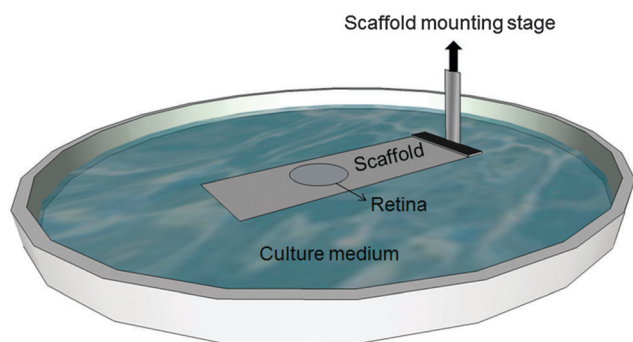

Fig. 1 Culture of guinea pig retina on TiO_2 scaffolds. The TiO_2 nanotube scaffold with the retina explant on top is placed in a Petri dish. A holder keeps the scaffold on the surface of the culture medium that the retina explant comes into contact with the medium but is not covered with liquid. During the entire experimental procedure, the holder connects the scaffold with the mechanical spectroscopy setup which is also placed inside a tissue culture incubator.
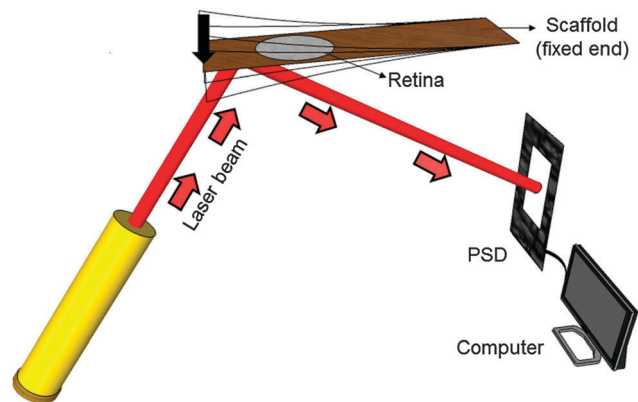

Fig. 2 Sketch of the setup for mechanical spectroscopy. The vibrating TiO_2 scaffold with the retina explant on top is pressed down once (arrow) to vibrate freely. A laser beam which is reflected on the scaffold's bottom side is detected using a position sensitive detector (PSD). An analog-digital converter is employed to record the signal.

During the experiment one end of the reed was clamped to the setup between two stainless steel plates. The free reed end was excited to vibrate by a plastic lever attached to a motor which pressed the free end down once. The resulting free damped oscillation of the scaffold was monitored by a laser beam reflected on a 5 mm × 5 mm silicon plate of 0.29 mm thickness glued to the bottom side of the scaffold. The position of the reflected beam was determined using a position sensitive detector (PSD 1L20-CP3, SiTek) that was read out – after a pre-amplification stage – by a computer using LabVIEW (National Instruments LabVIEW™ 2011 Signal-Express for DAQ) in combination with an analog-to-digital converter card (National Instruments NI USB-6009, sampling rate 48 kS per s). More details on these aspects of the hardware can be found in our previous publications.[26,28]

2.4. Experimental procedure

Prior to each experiment the vibrating reed setup was calibrated to ensure that the laser beam, which is reflected on a non-vibrating reed, hits the PSD in the center under an angle of 90°. Subsequently, the setup was placed in a tissue culture incubator at 37 °C and in a humidified atmosphere. A plastic lever attached to a little motor was moved over the scaffold's free end and carefully pressed the scaffold down by approximately 5 mm. Then the incubator was closed and the incubator humidity and temperature were equilibrated for 5 minutes. The lever was then moved away from the scaffold which generated free damped oscillations. All electronic devices of the setup were connected to power supplies outside the incubator. Moreover, all devices could be operated from outside the incubator without opening it.

To investigate the mechanical properties of the retina with the TiO_2 scaffold as a vibrating reed, the following experimental procedure was performed: (i) the vibration frequency of the empty scaffold inside the incubator was measured as described above. (ii) A Petri dish holder with a culture medium filled Petri dish was placed inside the incubator under the scaffold overnight (see Fig. 1) to investigate possible effects of medium on the scaffold's vibration frequency. The next day the Petri dish was removed and

medium on the scaffold was aspirated. Subsequently, the vibration frequency of the reed was determined as described in (i). (iii) A circularly punched retina explant was placed on top of the scaffold with the photoreceptor side down as sketched in Fig. 1. A Petri dish with culture medium was placed under the scaffold that the retina was in contact with fresh medium but not covered with liquid. The entire setup was incubated overnight that the retina could adhere to the scaffold. Afterwards the Petri dish was removed and all liquid was aspirated. Immediately the vibration frequency of the reed with tissue on top was measured as described before.

Each experimental step (i)–(iii) was repeated 5 times. The resulting oscillation curves were analyzed using Origin Pro 8G software to gain the vibration frequencies of the scaffolds. From the frequencies of (i) the empty scaffold, (ii) the scaffold after contact with culture medium and (iii) with retina tissue on top, the elastic properties, *i.e.* the Young's modulus, of the scaffold and the retina were determined by finite element calculations as described in the following.

2.5. Determination of experimental Young's moduli with the help of finite element calculations

Effective Young's modulus calculations of empty TiO$_2$ nanotube scaffolds, scaffolds after contact with culture medium and retina explants on top were carried out based on finite element analysis. The geometry and material properties of empty scaffolds with a silicon reflector and scaffolds with a reflector and retina on top were determined from the experiment and applied to create the scaffold model for finite element calculations by using COMSOL Multiphysics® 4.1 as shown in Fig. 3.

The TiO$_2$ scaffold was modeled as one effective material with an unknown Young's modulus and an effective density of 4234 kg m^{-3}. It results from a titanium density of 4507 kg m^{-3} and a density of the two 5.9 μm thick nanotube layers of 1095 kg m^{-3}.[26] All other materials parameters for the silicon reflector were taken from the Comsol database. For the retina a thickness of 120 μm[29] and a density of 1017 kg m^{-3} were employed,[30] as well as a Poisson ratio of 0.49.[31]

According to the experiment, one end of the modeled scaffold was fixed while the other end was kept free. Free tetrahedral structural solid finite elements were defined before

generating an extremely fine mesh where the scaffold was discretized into 84 851 elements.

In the first step, the elastic properties of the empty scaffold were determined by iteratively changing the Young's modulus until the resulting vibration frequency of the modeled scaffold matched the measured frequency from the experiment. Second, we assume that the dimensions of the reed – especially its thickness – did not change after contact with culture medium. We modeled the scaffold with identical parameters as before but with varied mechanical properties due to a differently measured frequency. By changing the Young's modulus as described before, we obtained the new scaffold's modulus when the frequency in the calculation matched the measured value. Third, the retina explant was modeled on the scaffold at the position identical to the experimental procedure. We employed the Young's modulus of the scaffold as determined before from experiments in culture medium as reference and changed the Young's modulus of the modeled retina until we reached the frequency we observed in experiments with retina explants on the scaffolds.

2.6. Profiles of protein adsorption on nanostructured scaffolds

To investigate possible interaction of culture medium including horse serum with TiO$_2$ nanotube scaffolds which might affect the vibration frequency, we analyzed protein adsorption from medium and serum on the scaffolds. In particular, adsorption of serum albumin, one major serum component which inhibits cell adhesion, and fibronectin, important for specific cell adhesion, was imaged employing immunostaining.

TiO$_2$ nanotube scaffolds were soaked in horse serum containing medium for 2 hours. Subsequently, scaffolds were taken out and washed with PBS twice. The primary antibodies consisting of sheep anti-horse albumin (Linaris biologische Produkte, cat. no. LAH0103) and rabbit anti-human fibronectin (Linaris biologische Produkte, cat. no. PAK0014) were diluted with 1% cold fish gelatin in PBS at a ratio of 1 : 100, added as a cocktail to the surface of the scaffolds (200 μl) and incubated at 4 °C overnight. The scaffolds were washed with PBS/gelatine three times and then incubated with Rhodamin-conjugated mouse anti-rabbit (Linaris biologische Produkte, cat. no. PAK0113) and FITC-conjugated donkey anti-sheep (Linaris biologische Produkte, cat. no. PAK0016) for 1 hour at 4 °C. Finally, the scaffolds were washed with PBS/gelatin three times and imaged using a Zeiss AxioScope fluorescence microscope.

3. Results

Viscoelasticity of condensed matter is generally reflected by the presence of elastic and dissipative contributions to mechanical response, as quantitatively cast into frequency dependent storage and loss moduli. While both are basically accessible by determining the frequency and temporal decay of a freely vibrating reed of length L, thickness d and density ρ, we presently focus on the Young's modulus E related to the oscillation frequency ω via:[32]

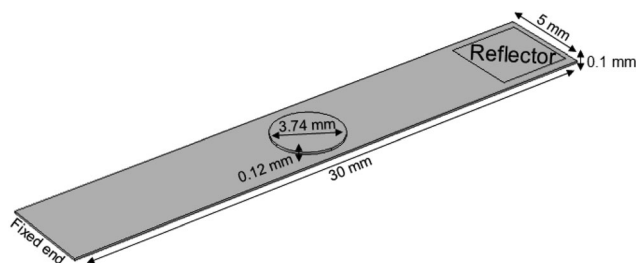$$E = \frac{\omega^2 \cdot 12\rho \cdot L^4}{1.875^4 \cdot d^2} \tag{1}$$

Fig. 3 Visualization of the scaffold model by finite element calculations. The retina explant (circular object on scaffold) was modeled at the same position as seen in the experiment. Scaffold, reflector (rectangular silicon plate glued on the bottom side of the scaffold) and retina dimensions are taken from experimental values.

For composite materials and vibrating reeds which consist of different material types, an analytical description of the relation between the Young's modulus and the frequency can be very challenging or even impossible to derive. Here we use mechanical spectroscopy with a self-designed setup to obtain the Young's modulus of retina wholemounts from the vibration modes of entire tissue explants.§ In our device a nanostructured TiO$_2$ scaffold acts as a vibrating support material for the retina which is excited to vibrate freely with the tissue on top. From the change in vibration frequency, the tissue's mechanical properties are extracted and analyzed by finite element calculations as described in the following.

3.1. Vibrating nanotube scaffolds for mechanical spectroscopy

A prerequisite for mechanical spectroscopy of tissue explants is a solid but an elastic support material as a scaffold which can be excited to vibrate freely as a reed with the tissue on top. Moreover, the tissue must be able to adhere to the scaffold without the addition of a glue that interferes with the mechanical properties of the scaffold and the tissue. Furthermore, the tissue must be viable and must not lose its organotypic structure. As we have shown previously, TiO$_2$ nanotube scaffolds of certain nanotube diameters combine all these needs.[27] When the retina is placed on top with the photoreceptor side down, the tissue automatically attaches to the nanotube surface while the entire organotypic structure is maintained over at least two weeks. Here we prepared nanostructured scaffolds with tube diameters of around 70 nm by anodization, as depicted in Fig. 4.

For mechanical spectroscopy of the retina the nanotube scaffold with the tissue on top is clamped into a holder. A plastic lever presses the scaffold's flexible end down once to excite free damped oscillations. A laser beam which is reflected on a small piece of silicon on the scaffold's bottom side hits a PSD which converts an electric signal into a position of the scaffold to directly derive its oscillation behavior as shown in Fig. 4 (for more details see the Experimental section).

As can be seen, the reed vibrated with a damped sinusoidal oscillation. However, we first tested and calibrated the new setup by first using a pure titanium sheet (23.5 mm × 10.5 mm × 0.1 mm) as a vibrating reed without retina on top. A silicon plate (5 mm × 5 mm × 0.29 mm) was employed as a reflector for the laser beam and glued on the bottom side of the reed at the flexible end. The reed was excited to vibrate freely on air, and a frequency of 108 ± 1 Hz was found. Even after five independent experimental runs the oscillation frequency remained constant and fully reproducible. We also employed a Fourier analysis of the measured vibration frequencies to determine the excited modes of the scaffold. It turned out that only the first mode was excited as expected.

§ As our test measurements indicate, damping behavior can reliably only be evaluated when working in a vacuum. As the latter are incompatible with organotypic culture for obvious reasons, we refrain from the evaluation of the latter.

To confirm the working principle of the setup, we analyzed the vibration of a titanium reed with a silicon reflector of the same dimensions using finite element calculations. We obtained the identical vibration frequency which confirms our combined experimental-computational approach.

In contrast to pure titanium, TiO$_2$ nanotube scaffolds showed lower vibration frequencies because of different material properties as described previously.[26] Since the mechanical spectroscopy measurements with the retina were performed in humidified air in a tissue culture incubator, we additionally tested effects of humidity. For a 22 mm long scaffold we found a vibration frequency in humidified air inside the incubator at 37 °C of 102.0 Hz, which is only 0.2% reduced compared to experiments outside the incubator at room temperature. The outcome was also confirmed by additional experiments with other scaffold lengths.

Since the frequencies ω we measured are directly related to the nanotube scaffold length l described in detail in ref. 26, we found the lowest frequencies between 91 and 97 Hz for the longest scaffolds with lengths between 24.3 and 25.3 mm. For the shortest reeds with 18.4–19.2 mm length, frequencies between 147 and 162 Hz were determined (Fig. 5). From both experimental series – the pure reed and after contact with medium – we found a $\omega \propto \dfrac{1}{l^2}$ dependency in agreement with other studies.[26]

3.2. Effect of protein adsorption on vibration modes

Since the scaffold was in contact with culture medium including horse serum, which is necessary for tissue culture and supply of the retina with nutrients, effects of medium ingredients on the nanotubes were determined. When the scaffold was placed in culture medium overnight and the medium was aspirated before oscillation, the vibration frequency was consistently higher, with an average increase of 7.7 ± 0.7% for all employed scaffold lengths (see Fig. 5). The same increase was seen when the scaffold was in contact with 10% horse serum diluted in Millipore water before. In contrast, soaking the scaffold in water, PBS or pure culture medium overnight hardly changed the vibration frequency. Thus, salt deposition on the scaffold surface and surface tension effects from water, which might result in a changed vibration frequency, can be neglected. In contrast, effects from serum–scaffold interaction must be taken into account when analyzing the vibration frequency of the nanotube reed with tissue on top.

We analyzed protein adsorption on the scaffolds by SDS-PAGE (sodium dodecyl sulfate polyacrylamide gel electrophoresis) measurements together with densitometry analysis (see ESI†). For serum albumin – one of the major components of serum – we found that (4.54 ± 0.71) µg cm^{-2} albumin adsorbs on the nanotubes. Considering a recent study by Kulkarni *et al.* on the adsorption of serum proteins on TiO$_2$ nanotube scaffolds with geometries similar to ours,[33] serum proteins were found to adsorb on the nanotube walls inside the nanotubes and fill up the tubes, while only a small albumin layer below 4 µm thickness is expected on the nanotube surface as reported by
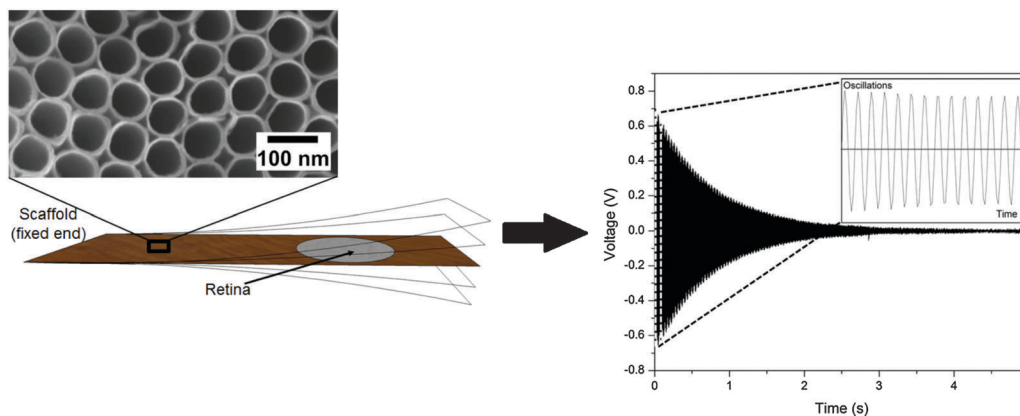
Fig. 4 Free damped oscillation of the TiO$_2$ nanotube scaffold. (left) The scaffold which acts as a vibrating reed is fixed at one end. The magnification of the reed shows a field emission scanning electron microscopy (FESEM) image of the scaffold surface which is a highly ordered array of parallel aligned nanometer sized tubes created by the anodization process. A lever presses the flexible end down (arrow) to excite the reed to oscillate freely. A laser beam is reflected on a silicon plate attached to the reed's bottom to a position sensitive detector which records the oscillation (the magnification showing the first 14 oscillations) as a voltage change with time (right). During mechanical spectroscopy of the retina, a tissue explant is placed on the scaffold as depicted on the left.
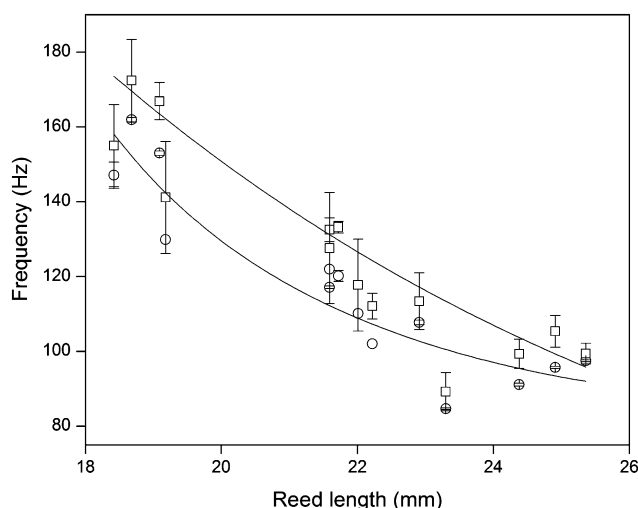

Fig. 5 Reed length influences scaffold frequency. For various nanotube scaffold lengths l different vibration frequencies ω are obtained. (□) Shows measured frequencies of the reed in a humidified atmosphere inside the incubator, and (○) frequencies of the nanotube reed after soaking in culture medium overnight. Data are fitted with $\omega = \dfrac{1}{al^2}$ (a = const.) according to eqn (1).

Wehmeyer *et al.*[34] Thus, for the obtained albumin density, more than 2200 albumin molecules adsorb inside one nanotube besides other serum proteins which are not investigated here. In contrast, no protein adsorption was seen for pure titanium sheets.

As an example of protein adsorption, Fig. 6 shows fluorescence images of albumin and fibronectin adsorbed on the nanotube scaffolds. Thus, protein adsorption results in the formation of a new composite material with TiO$_2$ nanotubes filled with serum proteins. This composite structure comprises completely new mechanical properties which result in changed intrinsic vibration frequencies of the reed that must be taken into account during mechanical spectroscopy of retina explants in contact with medium.

3.3. Mechanical spectroscopy of retina explants

After soaking the TiO$_2$ scaffold in medium overnight and measuring its resulting vibration frequency, the retina explant was placed on top of the scaffold. After tissue adhesion for another night, the vibration frequency of the scaffold with retina changed by about 1–2 Hz with respect to the frequency after protein absorption. This change is much smaller than effects from contact with medium, which might be attributed to the fact that the retina explant covered only a small fraction of the scaffold's surface in contrast to protein adsorption on the entire surface.

The same frequency of the reed with tissue was obtained when the scaffold was not kept in medium prior to tissue culture. Thus, we expect that protein adsorption occurs before the tissue adheres to the nanotube scaffold. This adsorption is also the reason for the good attachment of the retina in contrast to pure titanium onto which neither protein adsorption nor retina adhesion was demonstrable.

3.4. Finite element calculations and mechanical property analysis

Finite element calculations were employed to determine the elastic properties of the nanotube scaffolds and the retina explants from the measured vibration frequencies (Fig. 7). Since the nanotube scaffold is composed of three layers (5.9 μm nanotubes, 88.2 μm titanium and 5.9 μm nanotubes,
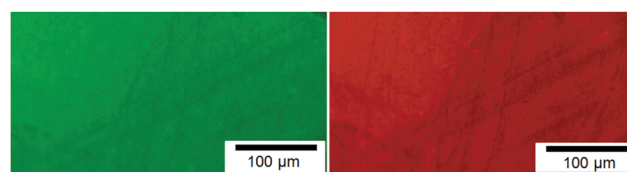

Fig. 6 Fluorescence images of protein adsorption on nanotube scaffolds. Fibronectin (left) and albumin (right) from horse serum.

see Methods and materials), simulation of such a reed structure takes enormous computational effort in terms of meshing because the nanotube layers are extremely thin compared to the reed length. Thus, we decided to model an effective reed consisting of only one material with the Young's modulus as a fitting parameter, as described in the Experimental section.

First, the effective Young's modulus of the empty TiO_2 reed was modeled by changing the Young's modulus of the material iteratively until the vibration frequency of the experiment of the empty nanotube scaffold was reached. Here we determined an average value of the effective Young's modulus of 80.4 ± 3.3 GPa. In this context we would like to annotate that eqn (1) cannot be employed to calculate the empty reed's Young's modulus from the measured frequencies analytically since the reflector plate on the reed's bottom side also has to be considered.

Second, we assumed that the layer of proteins on top of the nanotube scaffold is thinner than 4 nm as reported by Wehmeyer et al.,[34] and that the nanotubes are completely filled with serum proteins as recently shown by Kulkarni et al.[33] and corroborated by our SDS-PAGE/densitometry analysis. Thus, we modeled the reed after protein adsorption with the same parameters as before (even the reed density changed only by about 0.1%) and varied the new effective reed Young's modulus until we found the experimental frequencies. It turned out that the effective Young's modulus increased by $15.4 \pm 0.3\%$ to $E_{\text{eff}} = 92.8 \pm 3.6$ GPa compared to the empty scaffold.

The individual Young's moduli of the scaffold after protein adsorption were then employed as effective reed moduli when the retina was modeled on top of it. All the properties of the retina in terms of dimensions and Poisson ratio were determined from experiments and the literature (see Experimental). In the calculations the Young's modulus of the retina was also iteratively changed to find the experimentally matching vibration frequency. As a result an average retina's Young's modulus of 3.9 ± 2.6 GPa was found.

To study the effect of protein adsorption on the mechanical properties of the reed in more detail and to compare the protein stiffness with the obtained value for the retina, we employed sandwich beam analysis of a freely vibrating reed composed of three layers (for an overview see e.g. ref. 35). Since the nanotube layers on top and bottom of the reed are thin compared to the titanium core, the Young's modulus of the

nanotube layer including proteins can be derived from the effective Young's modulus of the entire reed E_{eff} and the Young's modulus of the titanium layer E_{Ti} by employing a modified (i.e. sandwich adapted) version of the Euler–Bernoulli beam theory, as described by Gryzagoridis et al.:[36]

$$E_{\text{NT+Prot}} = \left(\frac{E_{\text{eff}} l d^3}{12} - \frac{E_{\text{Ti}} l c^3}{12} \right) \bigg/ \left(\frac{l t^3}{6} + \frac{l t d^2}{2} \right), \qquad (2)$$

where l denotes the entire reed length and d is its thickness, c is the thickness of the titanium layer and t is the thickness of the nanotube layers which were determined from experiments. The effective modulus E_{eff} of the entire reed was taken from our finite element simulations and the modulus of titanium $E_{\text{Ti}} = 116$ GPa from the literature.[37] Here we obtained a Young's modulus of the protein filled nanotube layer of $E_{\text{NT+Prot}} = 37.3$ GPa.

Additionally, we used the Young's modulus of the filled nanotube layer to determine the modulus of the proteins within the tubes. To this end, finite element calculations on structural mechanics were performed on a nanotube model cell for a hexagonal tube arrangement (see Fig. 8 and ESI† for more details). Within the framework of linear elasticity, we applied a uniaxial stress acting on the nanotube walls. By varying the Young's modulus of the homogeneous protein filling, we obtained the correct value when the previously calculated effective Young's modulus of the nanotube layer including proteins matched the simulation results (Fig. S2 and S3, ESI†). Our finite element approach showed that the proteins within the nanotubes have a modulus of about $E_{\text{Prot}} = 15$ GPa. Moreover, for empty nanotubes $E_{\text{NT}} = 2.1$ GPa results (see ESI†) in excellent agreement with Fischer and Mayr.[26] Thus, protein
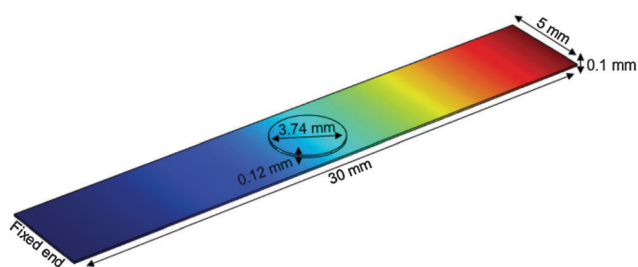

Fig. 7 Finite element calculation of freely vibrating nanostructured scaffolds with retina on top (circle). One end of the scaffold is fixed, while the other end vibrates freely. The color code shows the vibration amplitude from no extension (blue) to the maximum (red).
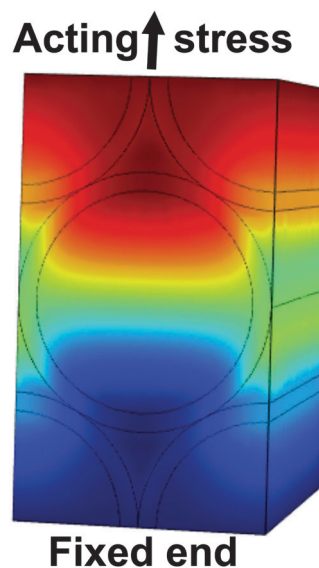

Fig. 8 Model cell of the hexagonal nanotube array (black lines) homogeneously filled with serum proteins. The bottom side of the cell was fixed, while a load of 100 MPa was acting onto the upper side parallel to the surface. The color-code denotes the displacement field ranging from -5.502×10^{-3} nm (dark blue) to 1.145 nm (dark red).

adsorption stiffens the nanotube layer by more than one order of magnitude.

4. Discussion

From biophysics and materials science point of view, the vertebrate retina is a very interesting tissue. It is the most light-sensitive biological tissue,[5,14] behaves like an elastic material and is always under tension *in vivo*[5,38] which can cause difficulties during surgery when the retina is cut and must be hindered to roll up and detach. The forces associated with retinal detachment depend on many factors such as pressure-driven flows, active retinal pigment epithelium (RPE) pump-mediated drag, cell–cell adhesion forces, and retinal tension forces.[39] The origin of the tension inside the retina is still unknown. The retinal structure and function are understood properly but its mechanical properties have not received great attention until now and are still a matter of debate.

Investigation of retinal mechanical properties was first employed by I. L. Jones *et al.*[38] who found a tissue's elastic modulus of 2×10^4 Pa for bovine retinae, while in this study the inhomogeneity of the retinal structure caused inaccuracies in the measurements. On the other hand Franze *et al.* used scanning force microscopy (SFM) to probe guinea pig retina mechanics on a micrometer length scale.[15] Here the retina elasticity was determined to be in the range of 940–1800 Pa, depending on the indentation position of the SFM tip. However, the elastic properties of the retina at different probing frequencies, as well as at molecular scales, are lacking.

To access frequency-dependent mechanical properties, magnetic resonance elastography (MRE) was established about 20 years ago.[40] Even though this technique has already been employed to investigate the frequency-dependent mechanical properties of neuronal tissue such as the entire brain,[41] only one study has addressed the elastic properties of ocular tissue so far. Litwiller *et al.* used MRE at a frequency of 300 Hz in combination with finite element modeling at a frequency of 300 Hz to probe the elasticity of the corneoscleral shell of an intact, enucleated bovine globe.[42] Estimated values of the Young's moduli of the cornea and sclera varied from 40 to 185 kPa and 1 to 7 MPa, respectively. However, no studies with varying frequencies and a specific investigation of the retina have been performed yet.

In our study the mechanical properties of adult guinea pig retina explants were probed in the range of about 85–172 Hz on freely vibrating TiO_2 nanotube scaffolds. Such nanostructured scaffolds, which have recently constituted an ideal substrate material for long-term culture of adult neuronal tissues,[27] support the strong adhesion of the cultured tissue on top, a prerequisite for organotypic culture and the investigation of tissue mechanics. The obtained retina's Young's modulus was found to be frequency independent in the probed range. Such constant Young's moduli of soft matter over even larger frequency ranges were confirmed by Lippert *et al.* who used 'wave-in-a-tube' ultrasonic methods to determine the mechanical

properties of brain tissue between 100 kHz and 10 MHz *in vitro*. Here the complex bulk modulus was fairly frequency invariant with values around 2133 MPa.[43]

In our experiments the maximum strain is reached directly at the beginning of the vibration when the reed is excited for the first time. We calculated the strain in terms of the deformation of single nanotubes on the reed's surface at the position of the retina when the reed vibrates. Here a 2 cm long reed which has an initial vibration amplitude of 0.125 cm at the center position of the retina exhibits a strain of 4% to the nanotubes. Since the retina is fully attached to the nanotube scaffold during vibration, the strain is directly transmitted to the tissue. For the determined small strain, we expect fully elastic behavior. Describing the retina as a viscoelastic material,[5] however, for fast deformation and small strains the retina behaves like an elastic solid in agreement with theoretical studies on tissue mechanics by Guevorkian *et al.*[44]

To quantify the elastic properties of the vibrating reed and the tissue on top, finite element calculations were employed. In contrast to the other – more macroscopic – studies on retina mechanics mentioned above, we found an unexpectedly high Young's modulus of the retina of 3.9 ± 2.6 GPa. This result cannot be explained by previous studies in which the exerted strain – *e.g.* by an indenting bead – results in a rearrangement of (sub-) cellular units and a compression or stretching of extracellular matrix (ECM) structures. During macroscopic deformation, intermolecular forces and the stiffness of the underlying biopolymer network and proteins are probed, which are orders or magnitudes smaller than our obtained value.[45–48] For instance, even for highly crosslinked collagen I gels, the entire gel stiffness would be below 8 kPa[49] – the same order of magnitude as the retina stiffness observed by Franze *et al.*[15]

A first hint that single biomolecules can influence the macroscopic mechanical properties of even solid metals in the range of GPa is given by our observation that proteins adsorbed from serum onto the nanotube scaffold increase the scaffold's Young's modulus by more than 15%. Such an effect was not seen when the scaffold was in contact with water or saline solution.

Two major components of serum are albumin, a globular protein of about 25 nm end-to-end distance in the expanded state[50] and fibronectin, a glycoprotein with 120–160 nm contour length,[51] which were both observed to adsorb onto the TiO_2 scaffold. Due to the super-hydrophilicity of the nanotube surface,[27] a droplet of culture medium including serum proteins immediately spreads and covers the entire scaffold such that protein adsorption results in a closed protein layer. Earlier spectroscopic ellipsometry measurements on TiO_2 nanostructured surfaces showed that the thickness of such adsorbed albumin proteins on the surface is below 4 nm,[34] while most proteins adsorb inside the nanotubes as shown recently by Kulkarni *et al.*[33] Together with our densitometry analysis we conclude that a composite material is formed consisting of more than 2200 serum albumin proteins filling each nanotube on the scaffold surface. Here, even "soft" proteins attached to a nanostructured thin layer on a macroscopic metal plate can

significantly change its mechanical properties in the range of GPa. In contrast we did not observe protein adsorption on flat titanium oxide sheets, in agreement with Oh *et al.*[52] and our previous study in which fibronectin absorption on metal substrates was found on the edges of microgrooves and not on polished surfaces.[53]

The question arises why a composite of solid TiO_2 nanotubes filled up with soft matter such as serum proteins yields a much higher Young's modulus compared to empty nanotube arrays. In fact, we employed sandwich beam theory and found that the Young's modulus of the nanotube layer increased from 2.1 GPa of the empty nanotubes to 37.3 GPa after protein adsorption. We expect that the similar dimensions of the nanotube diameter and the contour lengths of serum proteins play a key role in protein adsorption and the resulting stiffness. When the nanotubes are frequently stretched and compressed during vibration, the adsorbed proteins are stretched and compressed as well (Fig. 9). In contrast to intermolecular forces determining the tissue stiffness in the range of a few kPa, intramolecular forces are acting during the deformation of individual molecules which can be orders of magnitude higher. For instance, in 1936 Meyer and Lotmar performed the supposedly first theoretical calculation of the elastic behavior of polymers.[54] By using force constants obtained from spectroscopic data, the chain modulus of polyethylene and polyvinyl alcohol was estimated in the range of 250 GPa. Later experimental studies revealed that chain moduli of polyethylene terephthalate, polyparabenzamide, polyparaphenylene terephthalamide, polymetabenzamide and polypropylene are 121, 163, 182, 90, and 40 GPa, respectively.[54] Within the last decade biopolymers present in the ECM such as collagen, as well as filamentous assemblies connected with Alzheimer's disease and type II diabetes such as amyloid fibrils have been mechanically tested on the nanoscale.[55–57] All studies identified stiffness values of individual molecules in the range of GPa. In fact, collagen – one component of the ECM of the vertebrate retina[58] – was investigated by atomic force microscopy based techniques to study intramolecular forces and stiffness of individual collagen fibrils. Here van der Rijt *et al.* found stiffness values in the range of 2–7 GPa for dehydrated states,[55] while for low strains of 9%, a Young's modulus of 0.86 ± 0.45 GPa was determined in the wet state by Shen *et al.*[56] (for more examples on the Young's modulus of biological systems see ref. 59). Thus, we propose that the significant stiffening of the macroscopic nanotube scaffold after protein adsorption can be attributed to the high intramolecular forces acting at the nanometer length scale during the deformation of individual serum proteins when the

scaffold vibrates (Fig. 8). In fact, our finite element simulations of a nanotube model cell including a homogeneous protein filling reveal a protein stiffness of about 15 GPa.

The same effect can explain the high Young's modulus of the retina obtained in our experiments. Oh *et al.* found that prior to cell attachment on TiO_2 nanotube scaffolds, serum proteins adsorb as a prerequisite for cell adhesion.[52] However, the nanotubes are not "blocked" by these proteins, but cell protrusions are still able to adhere on the nanotube walls and even on the inside of the tubes.[52] Thus, we expect that the same stretching and compression of tissue molecules attached to the nanotubes result in the obtained high modulus of the retina in the range of GPa. Obviously, we probe the intramolecular forces of proteins and polymers from the cells of the outer photoreceptor layer and the interprotoreceptor (IPR) matrix in contact with the scaffold. This part of the retina and especially the IPR matrix is often involved in retinal detachment during pathological changes and is therefore of special importance in terms of tissue mechanics.[25,60] Here molecular variations during pathology lead to macroscopic changes of the retina that become visible in tissue rupture and loss of vision.

One possible candidate for the pathogenesis of retinal detachment is a dysfunction of chondroitin sulfate proteoglycan core proteins in the IPR matrix. These proteins are responsible for the adhesion of the neurosensory retina to the RPE[23–25] and are possible targets for new drugs against retinal tissue rupture and the formation of holes in the retina. With our assay it would also be possible to study the effect of drugs by functionalizing the scaffold surface with agents. The advantage of functionalization and coupling of agents directly to the nanotube scaffold would be that the agent is only supplied to the photoreceptor side of the tissue where it should act, and not to the entire tissue in case when the agent is directly supplied within the culture medium.

As the photoreceptor cells and the IPR matrix in contact with the nanotube scaffold involve many different molecular species including glycoproteins, proteoglycans, and hyaluronan,[24] it is not surprising that we obtained a relatively large error bar of the determined Young's modulus which reflects a variety of different elastic properties of the tissue at the tissue–scaffold interface at the nanometer scale. In summary, employing TiO_2 nanostructured scaffolds as vibrating reeds allows us to investigate the intramolecular elastic response of retinal tissue at the scaffold-tissue interface. In contrast to metals and metallic alloys, the mechanical properties of biomolecules depend on their structural conformation such as protein folding or unfolding. Our assay together with FRET[61] and fluorescence microscopy techniques with nanometer resolution such as STED[62] could offer new perspectives in studying changes in tissue mechanics in combination with optical inspections on the molecular level.

Fig. 9 Schematic representation of biomolecule adsorption on a TiO_2 nanotube surface. When the scaffold vibrates, biomolecules from the photoreceptor side of the retina such as proteins and polymers depicted in green and purple are stretched and compressed due to the acting strain of the underlying nanotubes (blue).

5. Conclusions and outlook

Solid TiO_2 nanotube scaffolds are ideal materials to probe the mechanical properties of neuronal tissue. They support strong adhesion of the tissue to their surface, a prerequisite for
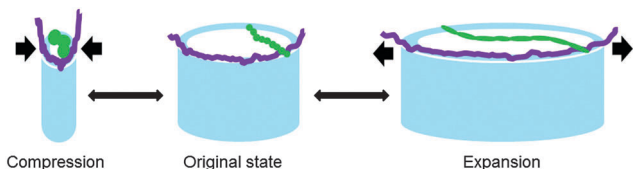
studying tissue elasticity at the scaffold-tissue interface. When the scaffold is employed as a freely vibrating reed with the tissue attached on top, the tissue proteins and polymers in direct contact with the nanotube surface are frequently stretched and compressed. Such strain results in elastic deformation of the tissue at the scaffold surface on the nanometer length scale. Together with finite element calculations we determined the stiffness due to acting intramolecular forces, which is of the order of a few GPa – only one order of magnitude smaller than the stiffness of the metal oxide scaffold.

Many eye diseases such as diabetic macular edema,[63] age-related macular degeneration[64] and retinoschisis are connected with mechanical failure, viz. the development of holes within the retina or the RPE, as well as detachment of the retina from the underlying RPE. Such detachment first occurs locally and then spreads within the tissue, a process which causes the loss of vision. How such local mechanical failure is related to stiffness variations on the single molecule level is still unclear. To this end, our approach of probing the mechanical properties at the nanoscale might open new perspectives in understanding tissue defects, and developing new drugs targeting these pathological alterations.

Our future work will focus on the detailed investigation of tissue–nanotube scaffold interaction important to understand tissue mechanics on the nanometer scale. We aim to understand which biomolecules adsorb to the nanotubes and how the tissue adheres to the nanostructured surface on the molecular level. Here a main focus will lie on the investigation of chondroitin sulfate proteoglycan core proteins of the IPR matrix which are supposed to be responsible for retinal adhesion. The dysfunction of such glycoconjugates and their correlation with mechanical properties on the molecular length scale can be addressed using our vibrating reed assay for a better understanding of retinal detachment.

Acknowledgements

References

1 L. V. Heilbrunn, *The Dynamics of Living Protoplasm*, Academic Press Inc., New York, 1956.

2 A. Fritsch, M. Höckel, T. Kiessling, K. D. Nnetu, F. Wetzel, F. M. Zink and J. A. Käs, *Nat. Phys.*, 2010, **6**, 730–732.

3 K. E. Kasza, A. C. Rowat, J. Liu, T. E. Angelini, C. P. Brangwynne, G. H. Koenderink and D. A. Weitz, *Curr. Opin. Cell Biol.*, 2007, **19**, 101–107.

4 A. E. Ekpenyong, G. Whyte, K. Chalut, S. Pagliara, F. Lautenschläger, C. Fiddler, S. Paschke, U. F. Keyser, E. R. Chilvers and J. Guck, *PLoS One*, 2012, **7**, 1–10.

5 K. Franze, *Development*, 2013, **140**, 3069–3077.

6 G. Beaune, T. V. Stirbat, N. Khalifat, O. Cochet-Escartin, S. Garcia, V. V. Gurchenkov, M. P. Murrell, S. Dufour and D. Cuvelier, *Proc. Natl. Acad. Sci. U. S. A.*, 2014, **111**, 8055–8060.

7 E. Schötz, M. Lanio, J. A. Talbot and M. L. Manning, *J. R. Soc., Interface*, 2013, **10**, 1–11.

8 M. Kohandel, S. Sivaloganathan, G. Tenti and K. Darvish, *Phys. Med. Biol.*, 2005, **50**, 2799–2805.

9 P. Friedl and K. Wolf, *J. Cell Biol.*, 2010, **188**, 11–19.

10 C. T. Mierke, *Phys. Biol.*, 2013, **10**, 1–21.

11 K. Franze, P. A. Janmey and J. Guck, *Annu. Rev. Biomed. Eng.*, 2013, **15**, 227–251.

12 T. Betz, D. Koch, Y. Lu, K. Franze and J. A. Käs, *Proc. Natl. Acad. Sci. U. S. A.*, 2011, **108**, 13420–13425.

13 M. F. Marmor, *Prog. Retinal Res.*, 1993, **12**, 179–204.

14 N. Lindqvist, Q. Liu, J. Zajadacz, K. Franze and A. Reichenbach, *Invest. Ophthalmol. Visual Sci.*, 2010, **51**, 1683–1690.

15 K. Franze, M. Francke, K. Günter, A. F. Christ, N. Körber, A. Reichenbach and J. Guck, *Soft Matter*, 2011, **7**, 3147–3154.

16 R. B. Mac Donald, O. Randlett, J. Oswald, T. Yoshimatsu, K. Franze and W. A. Harris, *J. Cell Biol.*, 2015, **210**, 1075–1083.

17 V. Brunetti, G. Maiorano, L. Rizzello, B. Sorce, S. Sabella, R. Cingolani and P. P. Pompa, *Proc. Natl. Acad. Sci. U. S. A.*, 2010, **107**, 6264–6269.

18 K. Franze and J. Guck, *Reports on Progress in Physics*, 2010, **73**, 094601.

19 A. N. Kapanidis and T. Strick, *Trends Biochem. Sci.*, 2009, **34**, 234–243.

20 M. Carrion-Vazquez, P. E. Marszalek, A. F. Oberhauser and J. M Fernandez, *Proc. Natl. Acad. Sci. U. S. A.*, 1999, **96**, 11288–11292.

21 K. Limmer, D. A. Pippig, D. Aschenbrenner, H. E. Gaub and F. Leng, *PLoS One*, 2014, **9**, 1–6.

22 A. Engel, H. E. Gaub and D. J. Müller, *Curr. Biol.*, 1999, **9**, 133–136.

23 G. S. Hageman, M. F. Marmor, X. Y. Yao and L. V. Johnson, *Arch. Ophthalmol.*, 1995, **113**, 655–660.

24 J. G. Hollyfield, M. E. Rayborn, R. J. Midura, K. G. Shadrach and S. Acharya, *Exp. Eye Res.*, 1999, **69**, 311–322.

25 N. G. Ghazi and W. R. Green, *Eye*, 2002, **16**, 411–421.

26 K. Fischer and S. G. Mayr, *Adv. Mater.*, 2011, **23**, 3838–3841.

27 V. Dallacasagrande, M. Zink, S. Huth, A. Jakob, M. Müller, A. Reichenbach, J. A Käs and S. G Mayr, *Adv. Mater.*, 2012, **24**, 2399–2403.

28 S. G. Mayr and K. Samwer, *Phys. Rev. Lett.*, 2001, **87**, 1–4.

29 R. G. Buttery, C. F. Hinrichsen, W. L. Weller and J. R. Haight, *Vision Res.*, 1991, **31**, 169–187.

30 I. Fatt and B. A. Weissman, *British Library Cataloging-in-publication data*, 2nd edn, 1992.

31 I. A. Sigal, J. G. Flanagan and R. Etbier, *Invest. Ophthalmol. Visual Sci.*, 2005, **46**, 4189–4199.

32 A. S. Nowick and B. S. Berry, *Anelastic Relaxation in Crystalline Solids*, Academic Press, New York and London, 1972.

33 M. Kulkarni, A. Flašker, M. Lokar, K. Mrak-Poljšak, A. Mazare, A. Artenjak, S. Čučnik, S. Kralj, A. Velikonja,

P. Schmuki, V. Kralj-Iglič, S. Sodin-Semrl and A. Iglič, *Int. J. Nanomed.*, 2015, **10**, 1359–1373.

34 J. L. Wehmeyer, R. Synowicki, R. Bizios and C. D. García, *Mater. Sci. Eng.*, 2010, **30**, 277–282.

35 D. Backström and A. Nilsson, Flexural Vibrations af A Three-Layer Sandwich Beam, *Sandwich Structures 7: Advancing with Sandwich Structures and Materials*, Springer, Netherlands, 2005.

36 J. Gryzagoridis, G. Oliver and D. Findeis, *Insight*, 2015, **57**(3), 140–143.

37 http://webelements.com, last assessed Jan 2016.

38 I. L. Jones, M. Warner and J. D. Stevens, *Eye*, 1992, **6**, 556–559.

39 T. Chou and M. Siegel, *Phys. Biol.*, 2012, **9**, 1–9.

40 R. Muthupillai, D. J. Lomas, P. J. Rossman, J. F. Greenleaf, A. Manduca and R. L. Ehman, *Science*, 1995, **269**, 1854–1857.

41 J. Guo, S. Hirsch, A. Fehlner, S. Papazoglou, M. Scheel, J. Braun and I. Sack, *PLoS One*, 2013, **8**, 1–10.

42 D. V. Litwiller, S. J. Lee, A. Kolipaka, Y. K. Mariappan, K. J. Glaser, J. S. Pulido and R. L. Ehman, *J. Magn. Reson. Imaging*, 2010, **32**, 44–51.

43 S. A. Lippert, E. M. Rang and M. J. Grimm, *Biorheology*, 2004, **41**, 681–691.

44 K. Guevorkian, M. Colbert, M. Durth, S. Dufour and F. Brochard-Wyart, *Phys. Rev. Lett.*, 2010, **104**, 1–4.

45 F. Li, S. D. Redick, H. P. Erickson and V. T. Moy, *Biophys. J.*, 2003, **84**, 1252–1262.

46 J. Wong, A. Chilkoti and V. T. Moy, *Biomol. Eng.*, 1999, **16**, 45–55.

47 M. Rief and H. Grubmüller, *ChemPhysChem*, 2002, **3**, 255–261.

48 D. C. Lin, E. K. Dimitriadis and F. Horkay, *J. Biomech. Eng.*, 2006, **129**, 430–440.

49 S. Lin and L. Gu, *Materials*, 2015, **8**, 551–560.

50 D. C. Karter and J. X. Ho, *Adv. Protein Chem.*, 1994, **45**, 153–196.

51 H. P. Erickson, N. Carrell and J. McDonagh, *J. Cell Biol.*, 1981, **91**, 673–678.

52 S. Oh, K. S. Brammer, Y. S. Julie Li, D. Teng, A. J. Engler, S. Chien and S. Jin, *Proc. Natl. Acad. Sci. U. S. A.*, 2009, **106**, 2130–2135.

53 A. C. De Luca, M. Zink, A. Weidt, S. G. Mayr and A. E. Markaki, *J. Biomed. Mater. Res.*, 2015, **103**, 2689–2700.

54 I. M. Ward, *Structure and Properties of Oriented Polymers*, Springer science, published by applied science publisher ltd, 1975.

55 J. A. J. Van der Rijt, K. O. van der Werf, M. L. Bennink, P. J. Dijkstra and J. Feijen, *Macromol. Biosci.*, 2006, **6**, 697–702.

56 Z. L. Shen, M. R. Dodge, H. Kahn, R. Ballarini and S. J. Eppell, *Biophys. J.*, 2008, **95**, 3956–3963.

57 J. F. Smith, T. P. J. Knowles, C. M. Dobson, C. E. MacPhee and M. E. Welland, *Proc. Natl. Acad. Sci. U. S. A.*, 2006, **103**, 15806–15811.

58 P. A. Campochiaro, J. A. Jerdan and B. M. Glaser, *Invest. Ophthalmol. Visual Sci.*, 1986, **27**, 1615–1621.

59 S. Perticaroli, J. D. Nickels, G. Ehlers, H. O'Neill, Q. Zhange and A. P. Sokolov, *Soft Matter*, 2013, **9**, 9548–9556.

60 M. Ishikawa, Y. Sawada and T. Yoshitomi, *Exp. Eye Res.*, 2015, **133**, 3–18.

61 K. Truong and M. Ikura, *Curr. Opin. Struct. Biol.*, 2001, **11**, 573–578.

62 T. A Klar, S. Jakobs, M. Dyba, A. Egner and S. W. Hell, *Proc. Natl. Acad. Sci. U. S. A.*, 2000, **97**, 8206–8210.

63 T. Murakami and N. Yoshimura, *J. Diabetes Res.*, 2013, **2013**, 1–11.

64 M. Van Lookeren Campagne, J. LeCouter, B. L. Yaspan and W. Ye, *J. Pathol.*, 2014, **232**, 151–164.